Spectrum of CT Findings in Nonmalignant Disease of the Adrenal Gland[1]

Akira Kawashima, MD • Carl M. Sandler, MD • Elliot K. Fishman, MD • Chusilp Charnsangavej, MD • Kotaro Yasumori, MD Hiroshi Honda, MD • Randy D. Ernst, MD • Naoki Takahashi, MD • Bharat K. Raval, MD • Kouji Masuda, MD • Stanford M. Goldman, MD

CME FEATURE

This article meets the criteria for 1.0 credit hour in category 1 of the AMA Physician's Recognition Award. To obtain credit, see the questionnaire on pp 451-456.

LEARNING OBJECTIVES

After reading this article and taking the test, the reader will:

- Understand the spectrum of CT findings in benign conditions involving the adrenal glands.
- Be familiar with typical and atypical appearances of benign adrenal disease.
- Understand the use of CT for differentiating benign cortical adenoma from metastasis.

Computed tomography (CT) plays a leading role in the evaluation of nonmalignant disease of the adrenal gland. CT is highly accurate in the localization of adrenal masses in patients with diseases associated with hyperfunctioning adrenal glands such as Cushing syndrome and Cushing disease, Conn syndrome, adrenal tumors leading to virilization or feminization, and pheochromocytomas. CT permits a specific diagnosis of acute or subacute adrenal hematoma and myelolipoma. Hematomas are round to oval and have increased attenuation (50–90 HU) that decreases on follow-up CT scans. Myelolipomas typically manifest as a well-defined suprarenal mass with an attenuation of −30 to −115 HU. Adrenal cysts are usually round to oval and manifest as a hypoattenuating mass with a smooth, thin wall. CT is useful in the evaluation of patients with Addison disease, particularly the subacute form secondary to tuberculosis or disseminated histoplasmosis. Findings typically include bilateral adrenal enlargement with a central necrotic area of hypoattenuation and peripheral enhancement. Thin-section unenhanced CT permits accurate measurement of attenuation and can be used to differentiate adrenal adenoma from metastasis in a cancer patient with an indeterminate mass: Attenuation of 10 HU or less usually indicates adenoma rather than cancer. If the mass is found incidentally at contrast material–enhanced CT, delayed scans obtained as early as 5–15 minutes after intravenous administration of contrast material appear to have comparable accuracy.

Abbreviation: ACTH = adrenocorticotropic hormone

Index terms: Adrenal gland, CT, 86.1211 • Adrenal gland, cysts, 86.31 • Adrenal gland, diseases, 86.2053, 86.23, 86.54 Adrenal gland, hemorrhage, 86.546 • Adrenal gland, neoplasms, 86.31, 86.328 • Pheochromocytoma, 86.328

RadioGraphics 1998; 18:393–412

[1]From the Department of Radiology, Lyndon B. Johnson General Hospital, 5656 Kelley St, Houston, TX 77026 (A.K., C.M.S., R.D.E.); the Departments of Radiology (A.K., C.M.S., R.D.E., N.T., B.K.R., S.M.G.) and Urology (C.M.S., S.M.G.), University of Texas–Houston Medical School; the Russell H. Morgan Department of Radiology and Radiological Science, Johns Hopkins Medical Institutions, Baltimore, Md (E.K.F.); the Department of Diagnostic Radiology, University of Texas M.D. Anderson Cancer Center, Houston (C.C.); the Department of Radiology, National Kyushu Medical Center Hospital, Fukuoka, Japan (K.Y.); and the Department of Radiology, Kyushu University, Faculty of Medicine, Fukuoka, Japan (H.H., K.M.). Presented as a scientific exhibit at the 1996 RSNA scientific assembly. Received June 4, 1997; revision requested June 27 and received August 8; accepted August 19. **Address reprint requests to** A.K.

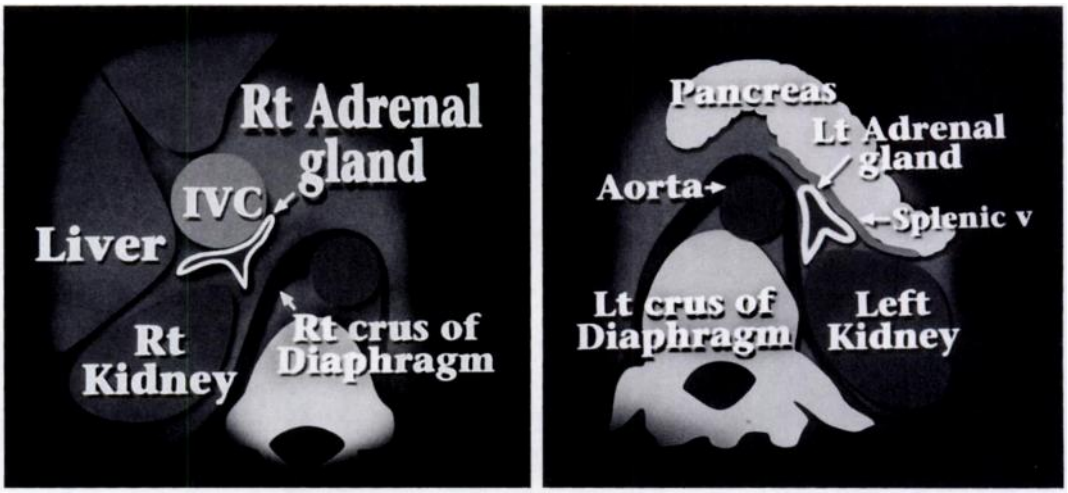

a. b.

Figure 1. Diagrams show normal cross-sectional anatomy of the right **(a)** and left **(b)** adrenal glands. *IVC* = inferior vena cava.

■ INTRODUCTION

Computed tomography (CT) plays a significant role in the radiologic evaluation of adrenal lesions (1,2). Adrenal masses are often discovered incidentally during the evaluation of a variety of abdominal complaints, and their presence has been reported in 0.5%–5% of all abdominal CT examinations (3,4). In addition, CT is the primary modality for localizing adrenal diseases that cause hyperfunction or hypofunction (5).

Recent articles on adrenal imaging have focused on the differentiation of benign adenomas from metastases (6–10). In this article, we present a comprehensive review of nonmalignant conditions of the adrenal glands. These conditions have been subdivided into three major categories: those characterized by hyperfunctioning adrenal glands, nonfunctioning adrenal glands, and adrenocortical insufficiency (ie, Addison disease). In addition, we describe our standard CT technique and normal adrenal anatomy, as well as illustrate key CT findings with representative cases.

■ CT TECHNIQUE

Routine CT with 7–10-mm collimation (depending on the scanner) can be used to image the adrenal glands. For a dedicated study, however, CT of the adrenal glands should be performed with 3–5-mm sections. Thinner sections must be used when smaller lesions are suspected and in all patients with Conn syndrome. From the raw scan data, a targeted reconstruction of the adrenal gland can be made with a smaller display field of view, which allows better spatial resolution.

Unenhanced studies are sufficient for the evaluation of conditions associated with adrenal hyperfunction. Unenhanced CT with thinner sections permits accurate measurement of attenuation and can be used to differentiate an adrenal adenoma from metastasis in a cancer patient with an indeterminate adrenal mass that has been demonstrated previously at routine contrast material–enhanced CT.

Acute to subacute hematomas can be seen at unenhanced CT and have a high attenuation that usually ranges from 50 to 90 HU.

The use of contrast material is sometimes helpful in characterizing an adrenal lesion in terms of the presence, degree, and pattern of

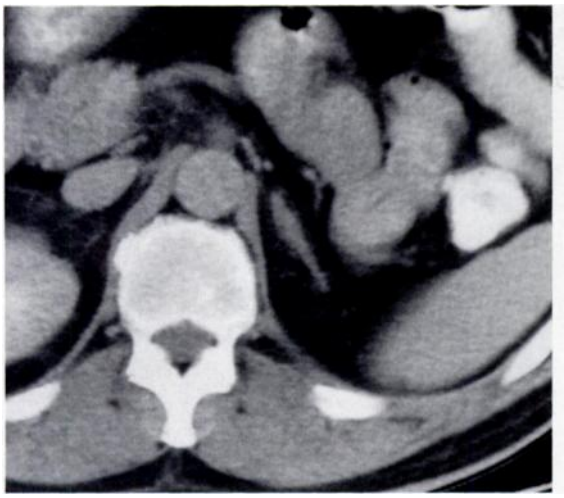

Figure 2. Left renal ectopy in a 40-year-old man. Contrast-enhanced CT scan reveals a linear rather than an inverted Y configuration of the ipsilateral adrenal gland (the "elongated adrenal" sign).

enhancement. Contrast-enhanced CT may also help determine the organ of origin of a mass when it is unclear from the unenhanced study whether the mass arises from the liver, the adrenal gland, or the kidney.

The value of helical (spiral) CT for evaluation of the adrenal gland has yet to be determined, but small lesions (<5 mm) should be easier to identify with this technique. Compared with conventional axial CT, multiplanar reformatted images generated from helical CT data permit more accurate localization of the lesion in relation to adjacent organs without misregistration.

■ NORMAL ADRENAL ANATOMY

The adrenal glands are located in the perirenal space, usually in a suprarenal position. Occasionally, however, an adrenal gland may be located anterior to the kidney, especially on the left side (Fig 1).

The right adrenal gland is located posterior to the inferior vena cava and medial to the liver. The gland is triangular at the top, but more caudally, it has an inverted V or Y shape. These projections are called the lateral (hepatic) and medial (crural) limbs. Using the inferior vena cava as a guide, one can identify the "split-tail tadpole" or "sperm" sign. The left adrenal gland is situated lateral to the aorta and posterior to the pancreas and splenic vein. Like the right adrenal gland, it has an inverted V or Y shape (the "Mercedes Benz" sign) inferiorly. In patients with renal agenesis or ectopy, the ipsilateral adrenal gland has a linear rather than an inverted Y configuration (the "elongated adrenal" sign) (Fig 2).

The adrenal gland is divided into the cortex and the medulla. The cortex is subdivided into three zones: the glomerular zone, which produces aldosterone; the fascicular zone, which produces cortisone; and the reticular zone, which produces androgens. The medulla is the site of catecholamine synthesis.

■ CONDITIONS ASSOCIATED WITH HYPERFUNCTIONING ADRENAL GLANDS

• Cushing Syndrome and Cushing Disease

Cushing syndrome is due to an excess of glucocorticoids from either exogenous or endogenous sources. The syndrome consists of truncal obesity, hirsutism, acne, moon face, facial plethora, purple striae, fatigue, weakness, hypertension, edema, impaired glucose tolerance, atherosclerosis, amenorrhea, and osteopenia. It is seen often in patients aged 30–40 years. Women are affected more frequently than men by a 4:1 ratio. Cushing disease, or adrenal hyperplasia due to overproduction of adrenocorticotropic hormone (ACTH), constitutes 70% of cases of endogenous Cushing syndrome. Cushing disease is caused by either a pituitary adenoma or, rarely, an ACTH-producing primary neoplasm elsewhere in the body.

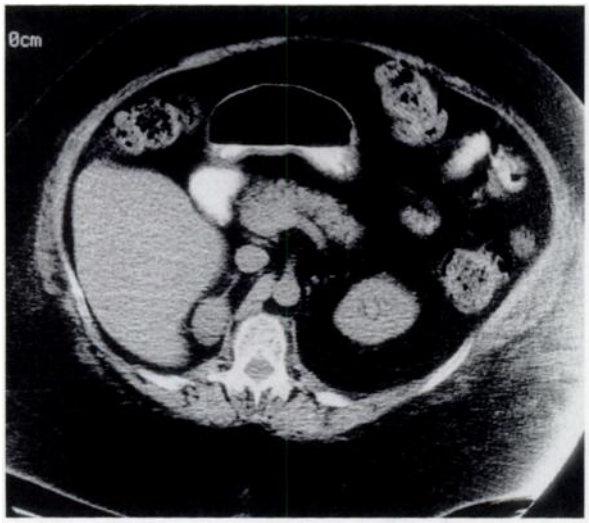

3.

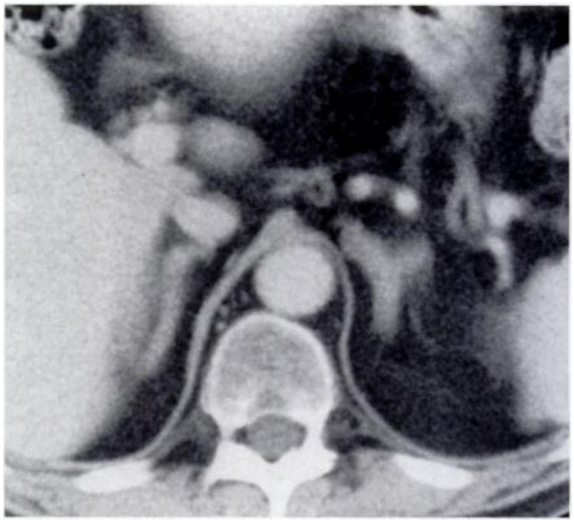

4.

5.

Figures 3–5. **(3)** Surgically proved hyperfunctioning adenoma in a 45-year-old woman with Cushing syndrome. Unenhanced CT scan demonstrates a well-defined, 2.5-cm-diameter oval mass arising from the posterior aspect of the right adrenal gland. Note the atrophy of a portion of the remainder of the gland projecting out from the adenoma as well as abundant fat. Demineralization of the vertebral body is better appreciated with the bone window setting (not shown). **(4)** Bilateral adrenal hyperplasia in a 49-year-old man with Cushing syndrome. Contrast-enhanced CT scan demonstrates symmetric enlargement of the adrenal glands. **(5)** Surgically proved massive macronodular adrenocortical disease in a 48-year-old man with Cushing syndrome. Contrast-enhanced CT scan reveals massively enlarged multinodular adrenal glands.

Cushing syndrome results from an adrenal adenoma in 20% of cases and from an adrenal carcinoma in 10% of cases.

In most cases, adrenal adenomas causing Cushing syndrome measure 2–4 cm in diameter. A hyperfunctioning cortical adenoma may be suspected at CT when a focal mass is present in one adrenal gland and the other gland is small (Fig 3). Adenocarcinoma is suggested when the mass is larger than 4 cm and central necrosis is present. In Cushing disease, there is bilateral, diffuse, uniform thickening of the adrenal glands (Fig 4); occasionally, there is bilateral macronodular enlargement. In long-standing disease, the adrenal glands can become nodular in appearance, a process known as multinodular hyperplasia (11). Although these lesions are usually ACTH-dependent, they are occasionally autonomous and quite large with multiple macronodules (Fig 5) (12). This entity is called massive macronodular hyperplasia and requires bilateral adrenectomy for treatment. Primary pigmented nodular adrenal disease, a rare cause of Cushing syndrome, is characterized by multiple small, pigmented adrenocortical nodules (13). This unusual entity may be familial and is associated with the Carney complex, which includes spotty skin pigmentation (lentigines), calcified Sertoli cell tumors of the testes, and cardiac and soft-tissue myxomas. Ectopic ACTH-producing primary neoplasms, a rare cause of Cushing disease, usually arise from the lung and mediastinum and include oat cell carcinoma and bronchial or thymic carcinoid. Chest CT has proved useful in diagnosing these lesions (14).

Figure 6. Surgically proved adenoma in a 65-year-old man with Conn syndrome. Unenhanced helical CT scan (4-mm collimation, 3 mm/sec table feed) reveals a well-defined, hypoattenuating mass arising from the lateral rim of the right adrenal gland. Note the atrophic portion of the remaining right adrenal gland projecting from the adenoma. The left adrenal gland is also atrophic.

• Conn Syndrome

Conn syndrome (primary aldosteronism) results in excess aldosterone production and may be caused by either adrenal adenoma or hyperplasia. Aldosteronomas are present in approximately 80% of cases, whereas bilateral adrenal hyperplasia is found in 20% of cases (15). Conn syndrome is characterized by hypotension, hypokalemia, and sodium retention. The hypokalemia manifests as muscle weakness, cardiac arrhythmia, carbohydrate intolerance, and nephrogenic diabetes insipidus.

Adenomas can be seen at CT in 70% of cases. In a recent review of aldosteronomas detected with CT, the average diameter was less than 2 cm (15). Therefore, CT should be performed with a collimation of 5 mm or less when Conn syndrome is the primary consideration. At CT, the adenoma appears as a hypoattenuating nodule in the adrenal gland (Fig 6). Among hyperfunctioning adenomas, aldosteronomas tend to have the lowest attenuation (15, 16). However, in a study by Doppman et al (17) of patients with surgically proved aldosteronomas, CT failed to reveal adrenal nodules in 50% of cases, resulting in a misdiagnosis of hyperplasia. With hyperplasia, the adrenal glands may be normal or may have a nodular or multinodular appearance. One or both adrenal glands may be enlarged. Medical therapy rather than surgery is usually indicated. When CT reveals normal adrenal glands bilaterally, bilateral nodules, or unilateral nodules with evidence of associated hyperplasia, correlation with functional studies is warranted for localization and characterization of the disease (17,18).

• Virilization and Feminization from Adrenal Tumors

Benign or malignant adrenal cortical tumors occasionally cause virilization or, rarely, feminization (1). Adrenal adenomas usually range from 2 to 6 cm in diameter and appear homogeneous, whereas carcinomas tend to be larger and appear heterogeneous. Adrenal virilization may result from congenital adrenal hyperplasia due to impaired cortisone or aldosterone synthesis secondary to an enzyme defect with increased ACTH stimulation by the pituitary gland (adrenogenital syndrome).

• Pheochromocytoma

Pheochromocytomas are tumors composed of chromaffin cells and may secrete catecholamines such as norepinephrine or epinephrine, causing elevated levels of catecholamine in the blood serum and urine. Alternatively, pheochromocytomas may be described as paragangliomas of the adrenal medulla. Urinary metanephrine or vanillylmandelic acid levels are elevated in over 90% of patients from whom 24-hour urine collections are obtained. Patients present clinically with hypertension, which may be paroxysmal, as well as palpitations, perspiration, and headaches. Pheochromocytomas have been called the "ten percent tumor": Approximately 10% are bilateral, 10% are extra-adrenal (paragangliomas of the retroperitoneum, mediastinum, or urinary bladder), 10% occur in children, and 10% are malignant. Pheochromocytomas are associated with multiple endocrine neoplasm syndrome, von Hippel-Lindau syndrome, and neurofibromatosis. These entities are usually associated with bilateral pheochromocytomas, some of which do

Figures 7, 8. **(7)** Pheochromocytoma in a 43-year-old woman with a family history of von Hippel-Lindau disease. Contrast-enhanced helical CT scan shows a 1-cm-diameter mass in the left adrenal gland (arrow) with marked contrast enhancement and a small hypoattenuating center. **(8)** Surgically proved bilateral pheochromocytomas in a 37-year-old man with a history of von Hippel-Lindau disease. **(a)** Contrast-enhanced CT scan demonstrates a large right adrenal mass with a cystic area (arrow) and a small left adrenal mass with punctate calcifications (arrowhead). **(b)** CT scan obtained through the kidneys reveals cysts (open arrows), a cystic mass (curved arrow), and a solid mass (straight solid arrow).

7.

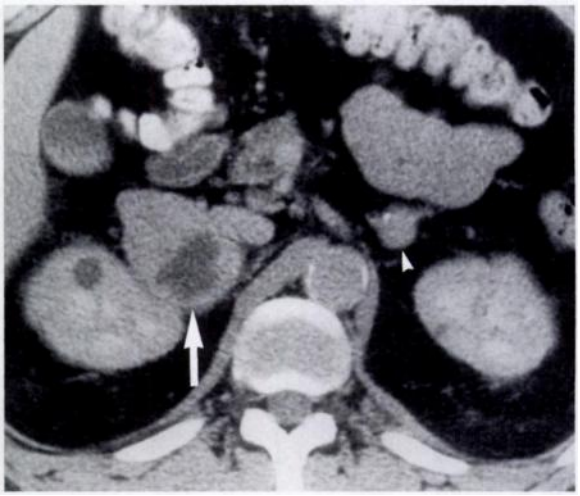

8a.

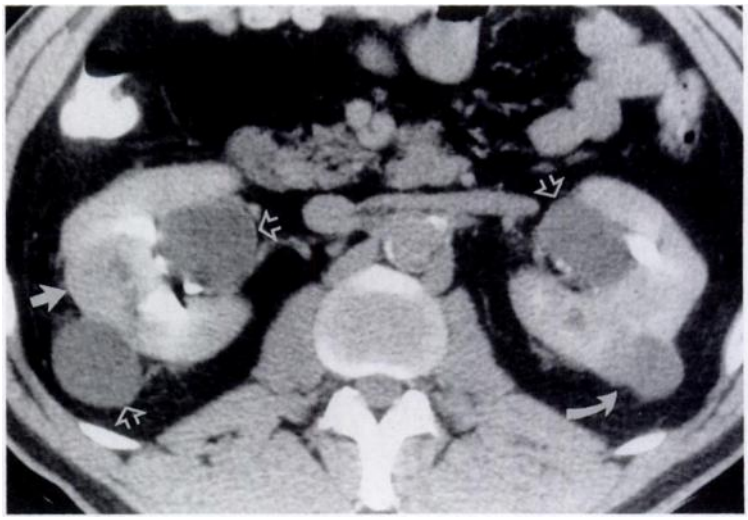

8b.

not produce abnormally high levels of catecholamine. The manifestations of the syndrome may not all occur simultaneously. Patients with sporadic pheochromocytomas may carry the gene for multiple endocrine neoplasm syndrome and von Hippel-Lindau syndrome but may have the adrenal tumor as its only manifestation (19).

At CT, pheochromocytomas are usually 3 cm or larger (Fig 7). Large pheochromocytomas are relatively cystic because of necrosis (Fig 8). Calcification is present in about 10% of cases. In patients with von Hippel-Lindau disease and multiple endocrine neoplasm syndrome, CT may reveal masses in the pancreas, kidney, and spinal cord (Fig 8). Pheochromocytomas are hypervascular tumors and exhibit marked enhancement after intravenous administration of contrast material (Fig 7). These studies should be performed with caution because some patients with pheochromocytoma have experienced a hypertensive crisis after administration of ionic iodinated contrast mate-

Figure 9. Bilateral adrenal hematomas in a 21-year-old man with a history of blunt abdominal trauma. **(a)** Contrast-enhanced helical CT scan reveals well-defined oval hematomas of both adrenal glands. Retroperitoneal hemorrhage is also present (arrows). Note the large hematoma and laceration in the right hepatic lobe with a perihepatic hematoma. **(b)** Follow-up enhanced CT scan obtained approximately 4 weeks later shows an interval decrease in the size and attenuation of the hematomas of the adrenal glands and the liver, as well as improvement of the periadrenal and perihepatic hematoma.

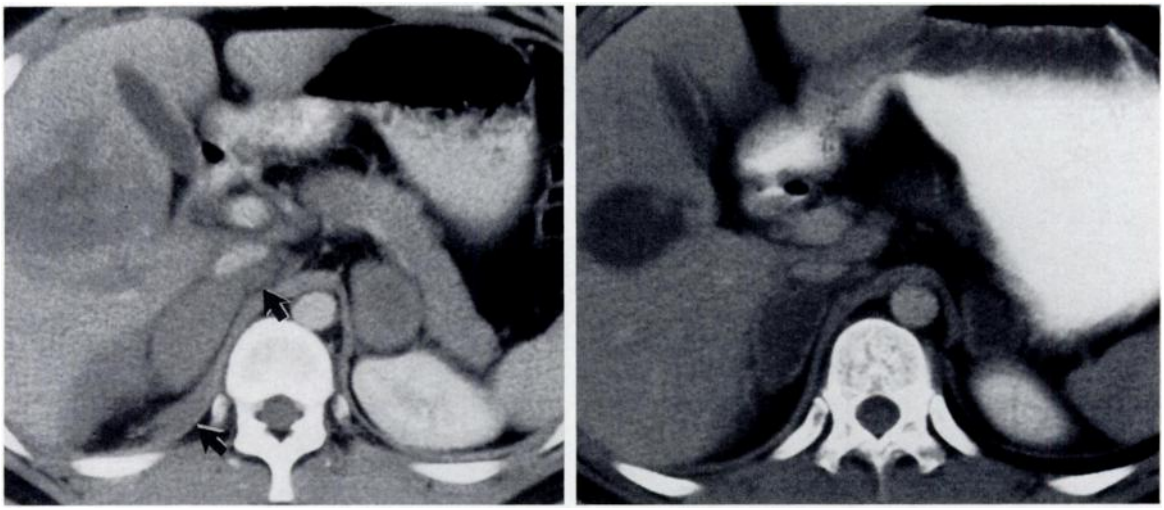

a. **b.**

rial. Some investigators have suggested that patients being evaluated for suspected pheochromocytoma be premedicated with an α-adrenergic blocking agent as a precaution against this complication (20,21). However, in a review of 20 cases of pheochromocytoma studied at the National Institutes of Health with nonionic contrast media but without adrenergic blockage, no adverse effects were observed (2). In a recent report by Mukherjee et al (22), no statistically significant elevation of serum epinephrine or norepinephrine levels was found in 10 patients with pheochromocytomas and six healthy control subjects after intravenous administration of iohexol for contrast-enhanced CT. Larger studies will be necessary to determine the safety of intravenous administration of nonionic iodinated contrast material in patients with pheochromocytomas.

■ CONDITIONS ASSOCIATED WITH NONFUNCTIONING ADRENAL GLANDS

• Hematoma

Traumatic Hematoma.—Adrenal injury occasionally occurs in the setting of multiple severe trauma. The prevalence of radiographically detected abnormalities is 2% (23), although adrenal injury has been reported in 28% of patients studied at autopsy who had sustained significant abdominal trauma (24). Adrenal hematomas resulting from blunt trauma arise in the medulla and stretch the cortex around the hematoma. Such hematomas manifest as a round to ovoid adrenal mass. The injury occurs in the right side in up to 90% of cases (25). This predilection has been attributed to direct compression of the gland by the spine and liver from blunt abdominal trauma, shearing of small vessels perforating the adrenal capsule by deceleration forces, and short-term rise in intraadrenal venous pressure due to compression of the inferior vena cava (23–26).

CT is the modality of choice for detecting adrenal injury, especially hematoma. The most common CT feature of adrenal injury is a round to oval adrenal hematoma (83% of cases) (Fig 9), followed by diffuse irregular hemorrhage obliterating the gland (9%) and uniform adrenal enlargement (9%) (23). Periadrenal hemorrhage is usually present and is evidenced by an ill-defined adrenal margin, periadrenal stranding, and asymmetric thickening of the diaphragmatic crus.

Hematomas vary in attenuation depending on their age. Acute to subacute adrenal hematomas have increased attenuation ranging from 50 to 90 HU. They gradually diminish in size, and there is a corresponding decrease in attenuation at follow-up CT. Calcifications may develop a few months after adrenal hemorrhage (27).

Adrenal biopsy may be necessary to differentiate adenoma from metastasis and has a high degree of accuracy (28). Furthermore, it is a safe procedure; major complications following adrenal biopsy have been reported in only 3% of cases (28). The most common complications are pain, bleeding resulting in an adrenal and periadrenal hematoma, and pneumothorax.

Hemorrhagic infarction and hematoma formation in the right adrenal gland have been reported in patients who undergo orthotopic liver transplantation and are attributed to ligation and division of the right adrenal vein during hepatectomy (Fig 10) (29).

Adrenal hematoma may occur as a result of adrenal venous sampling. A hematoma may also occur in the surgical bed after adrenectomy.

Nontraumatic Hematoma.—Spontaneous adrenal hemorrhage is usually associated with anticoagulant therapy (Fig 11) or with stress caused by surgery (Fig 12), sepsis, or hypotension (30). Most anticoagulant-associated adrenal hemorrhage occurs during the initial 3 weeks of treatment (31). Nontraumatic adrenal hematomas can be either unilateral (Fig 11) or bilateral (Fig 12). Like traumatic hematomas, they are round or oval and may contain perihemorrhage. The attenuation of these lesions at CT depends on the age of the hematoma.

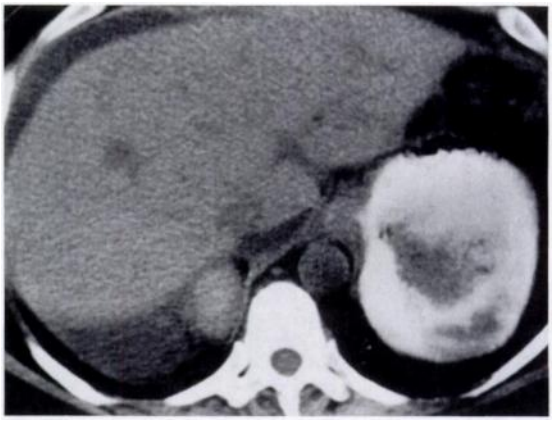

Figure 10. Adrenal hematoma in a 55-year-old woman who had undergone orthotopic liver transplantation. Unenhanced CT scan reveals a well-defined, hyperattenuating mass of the right adrenal gland, consistent with acute hemorrhage. The transplanted liver is surrounded by minimal ascites.

Spontaneous unilateral adrenal hemorrhage may be idiopathic but has been reported to be associated with an underlying adrenal condition such as a cyst, adenoma, hemangioma, myelolipoma, or metastasis (32).

• Cyst

Adrenal cysts are increasingly being detected incidentally at CT. Adrenal cysts are usually unilateral and solitary and have no side predilection. Most cysts are found in the 5th and 6th decades of life. The literature reports a 3:1 female preponderance (33). Patients with adrenal cysts are usually asymptomatic unless the cyst produces a mass effect on adjacent structures or is complicated by hemorrhage or infection.

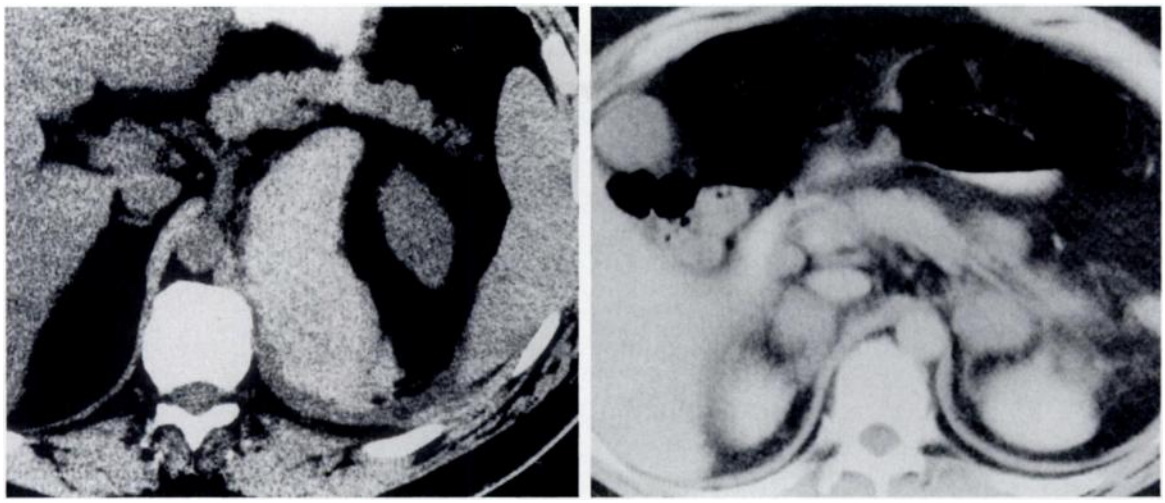

11. 12.

Figures 11, 12. **(11)** Adrenal hematoma in a 44-year-old man receiving coumarin for pulmonary emboli from deep venous thrombosis. Unenhanced CT scan reveals a large, high-attenuation hematoma of the left adrenal gland. **(12)** Bilateral adrenal hematomas in a 46-year-old man who had undergone splenectomy. Contrast-enhanced spiral CT scan reveals ill-defined hematomas of both adrenal glands associated with periadrenal stranding.

Nonparasitic adrenal cysts are divided into three categories on the basis of histologic findings: endothelial cysts (48% of cases), pseudocysts (42%), and epithelial cysts (10%) (33).

Endothelial cysts can be either angiomatous or lymphangiomatous. The latter are more common and are typically multiple small, 1–15-mm-diameter cysts or locules found incidentally at autopsy. Rarely, they may be solitary large, cystic lesions. Large lymphangiomatous endothelial cysts are also known as cystic lymphangiomas.

Pseudocysts represent the most common variety of adrenal cysts discovered clinically. The majority of these cysts are believed to result from hemorrhage and subsequent clot organization within a normal adrenal gland or an adrenal tumor. Septation, hemorrhage, or calcification may be present in pseudocysts.

Epithelial cysts include unusual cystic adenomas, glandular or retention cysts, and cystic transformation of embryonal remnants.

At CT, adrenal cysts typically manifest as a hypoattenuating mass with a smooth, thin wall (Fig 13). These cysts may be lobulated but are usually round or oval. The inferior wall of the

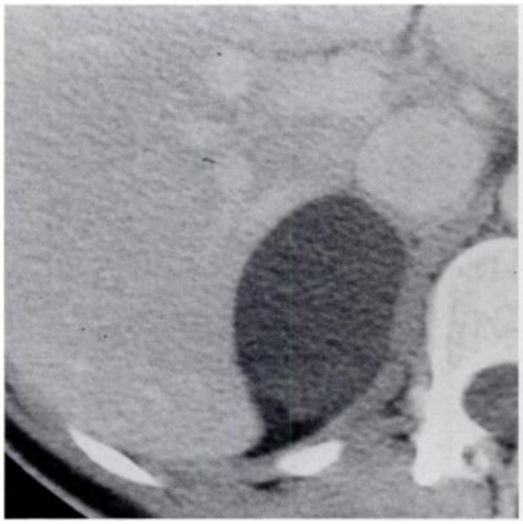

13a.

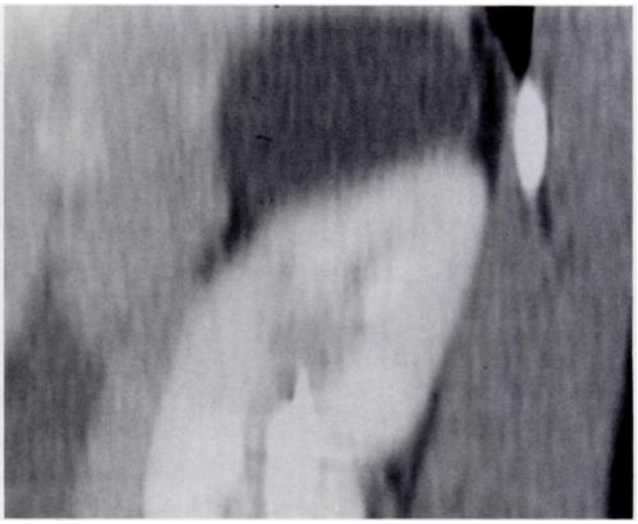

13b.

13c.

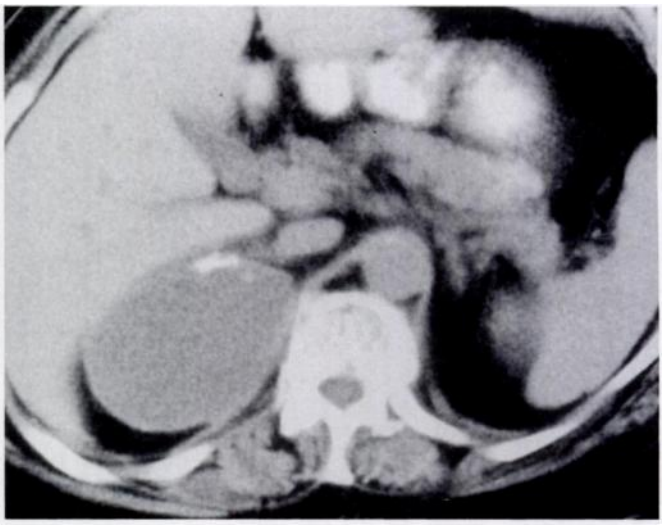

14.

Figures 13, 14. **(13)** Adrenal cyst in a 23-year-old woman who presented with abdominal pain. **(a)** Contrast-enhanced helical CT scan of the right adrenal gland shows a hypoattenuating mass of 8 HU. **(b)** Sagittally reformatted image reveals a relationship between the mass and the upper pole of the right kidney. **(c)** Transverse abdominal ultrasound (US) image reveals a sharply demarcated anechoic mass with increased through-transmission, indicative of a cyst. An unenhanced CT scan (not shown) obtained subsequently demonstrated a mass with an attenuation similar to that seen at enhanced CT (cf **a**). The patient continues to be followed up with no change in the appearance of the lesion. **(14)** Adrenal pseudocyst in a 66-year-old woman. Unenhanced helical CT scan reveals a large, well-defined hypoattenuating mass with a rim of calcification at the periphery.

mass is flat or concave. Radiologically, calcification is seen in adrenal cysts in 15% of cases and is often peripheral and curvilinear (Fig 14) (34). CT is more sensitive in detecting calcification than is conventional radiography. Cysts without calcification may be indistinguishable from adenomas because of their similar attenuation at CT. Both unenhanced and contrast-enhanced CT are of value in demonstrating the true nature of adrenal cysts because these cysts

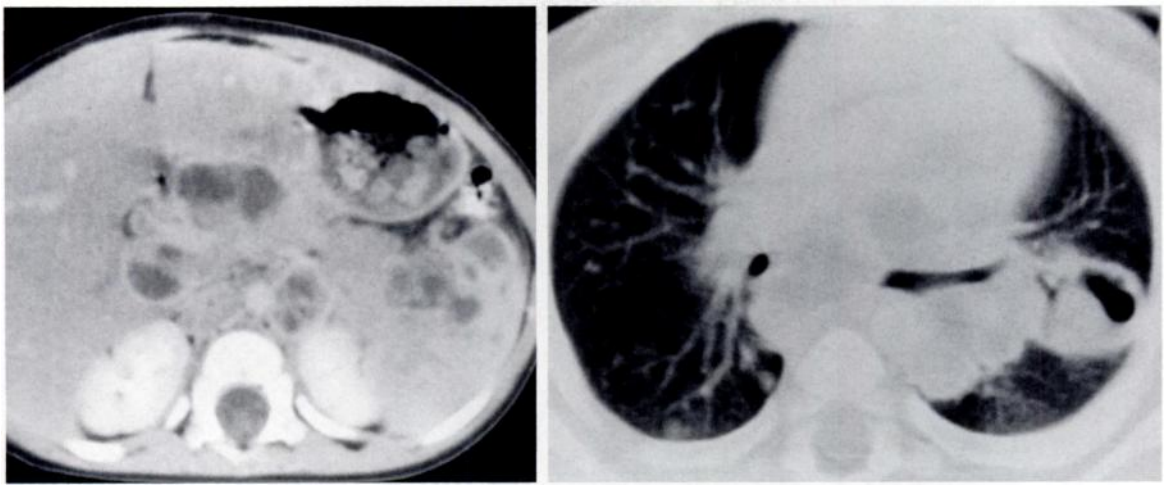

a. b.

Figure 16. Disseminated tuberculosis in a 12-month-old boy who failed to respond to conventional antitubercular therapy. **(a)** Contrast-enhanced CT scan reveals enlargement of the left adrenal gland, which contains hypoattenuating nodules and has a rim of enhancement. Note caseous lymphadenitis in the peripancreatic region and caseous granulomas in the spleen. **(b)** Contrast-enhanced CT chest scan obtained at the level of the hila with lung window settings demonstrates a left cavitary lesion and bilateral miliary nodules. Note left hilar and mediastinal adenopathy.

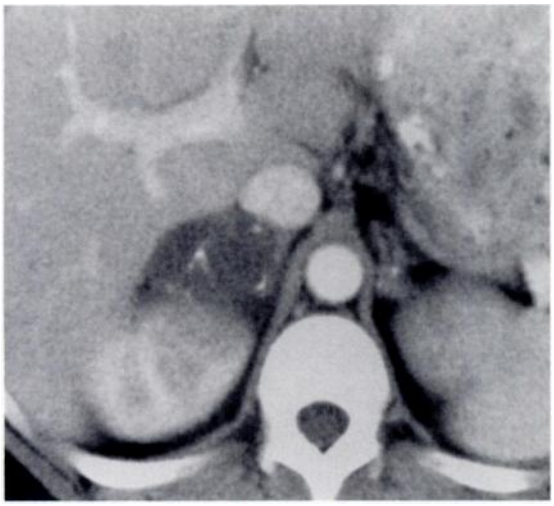

Figure 15. Surgically proved cystic lymphangioma of the adrenal gland in a 46-year-old woman. Contrast-enhanced spiral CT scan reveals a well-defined, multiloculated cystic mass. Scattered calcifications are present at the "pencil-thin" walls and septations.

do not enhance. In a recent report of 37 cases of benign adrenal cysts studied with CT, Rozenblit et al (35) found calcification in 20 cases (54%) and wall calcification (with or without central calcification) in 19 cases (51%). In less than 20% of cases, benign cysts demonstrated hyperattenuation (>60 HU) due to intracystic hemorrhage. Cystic lymphangiomas appear as a unilocular or multilocular cystic mass with an imperceptible wall (Fig 15).

When the wall is thickened or irregular, it is possible that the lesion represents hemorrhage into a benign or malignant tumor masquerading as a cystic mass. Clot in a hemorrhagic cyst may also appear as a solid component in the cystic mass. Interval change in the size and appearance of a solid component at serial imaging studies suggests the presence of a clot (36).

• Infections

Granulomatous Infection.—Tuberculosis is the most common infectious cause of Addison disease, accounting for 10%–30% of cases (37). The CT appearance of granulomatous infection depends on the time course and activity of the inflammatory process. CT findings of early tuberculous "adrenalitis" typically include bilateral adrenal enlargement with a central necrotic area of hypoattenuation and a peripheral enhancing rim (Fig 16) (37,38). In the healing stage of the disease, the adrenal glands become

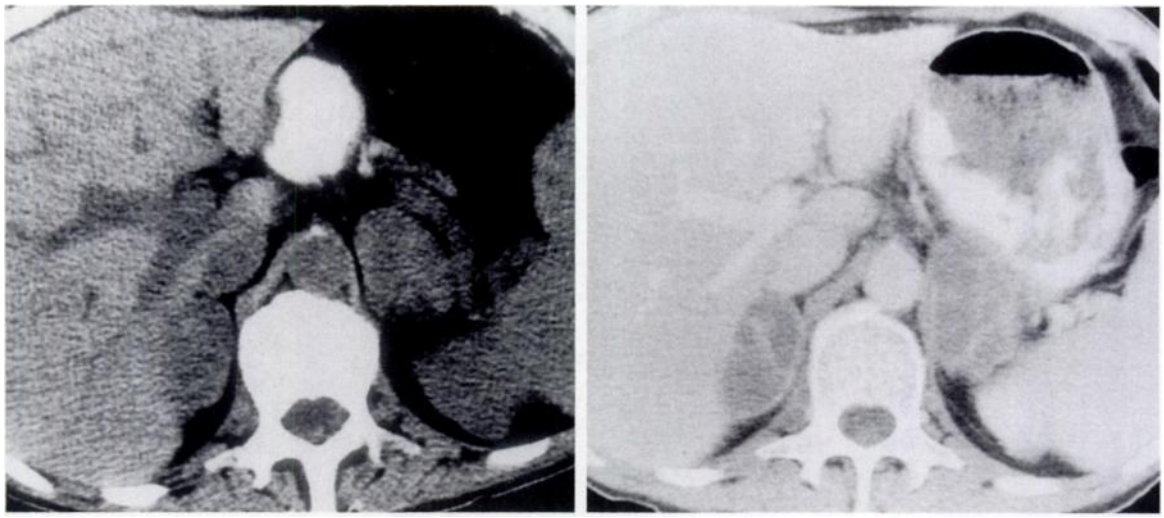

a. b.

Figure 18. Biopsy-proved disseminated histoplasmosis of the adrenal glands in a 64-year-old man who had undergone esophagectomy for esophageal cancer. **(a)** Unenhanced CT scan reveals enlargement of both adrenal glands. **(b)** Contrast-enhanced CT scan reveals that both adrenal glands have necrotic centers and a rim of contrast enhancement.

calcified and atrophic. However, its CT appearance is indistinguishable from that of other long-standing granulomatous infections, previous hemorrhage, and idiopathic adrenal calcifications (Fig 17).

Disseminated histoplasmosis usually occurs in endemic areas. It occurs in the setting of altered host immunity (eg, in patients with neoplasms and acquired immunodeficiency syndrome) (39). About 50% of patients with disseminated histoplasmosis ultimately develop Addison disease, and adrenal insufficiency due to histoplasmosis is invariably fatal if left untreated (40). The adrenal glands may be the only demonstrable sites of disseminated disease (41).

In disseminated histoplasmosis, CT typically reveals bilateral symmetric enlargement of the adrenal glands with central hypoattenuation and peripheral contrast enhancement (Figs 18, 19). The affected adrenal gland may contain variable amounts of calcification depending on the stage of the disease process. Disseminated histoplasmosis can be diagnosed at fine-needle aspiration biopsy, but the correct diagnosis may be missed unless special stains are used and the pathologist is alerted to the possibility of fungal infection (42).

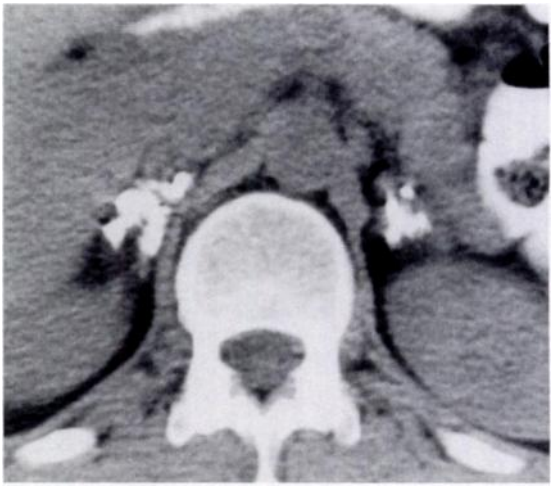

Figure 17. Idiopathic adrenal calcifications in a 35-year-old man with normal adrenal function. Unenhanced helical CT scan demonstrates coarse calcifications in the adrenal glands bilaterally, an appearance indistinguishable from that of other entities such as long-standing granulomatous infections and previous hemorrhage.

Pneumocystis carinii Infection.—Although *Pneumocystis carinii* is usually considered a respiratory pathogen, in immunocompromised patients such as those with acquired immunodeficiency syndrome, generalized dissemination of *P carinii* infection from the lungs may

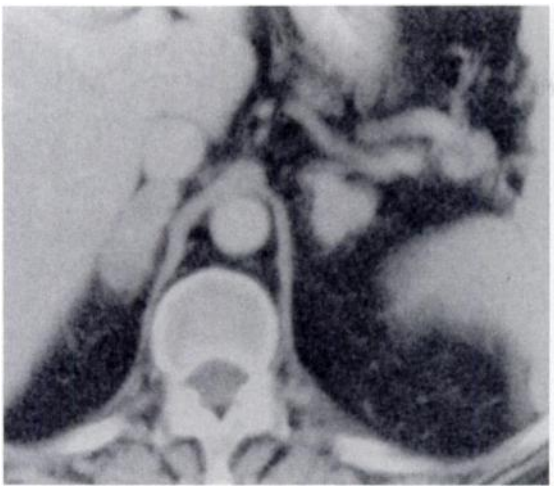

Figure 19. Disseminated histoplasmosis of the adrenal glands in a 57-year-old man with a history of Addison disease. Contrast-enhanced helical CT scan reveals enlargement of both adrenal glands. The diagnosis of disseminated histoplasmosis was established with biopsy of a nodule of the groin.

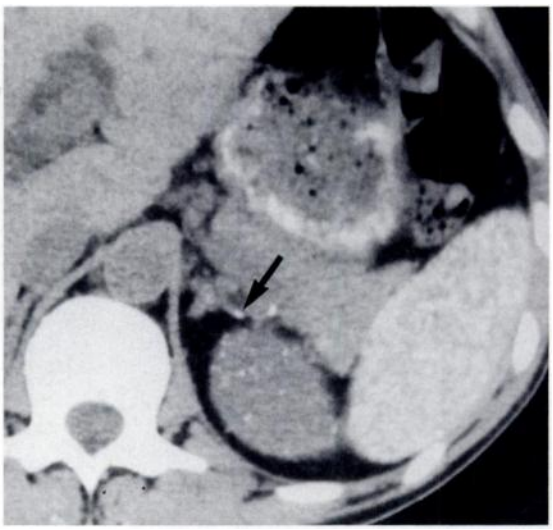

Figure 20. Disseminated *P carinii* infection in a 46-year-old man with acquired immunodeficiency syndrome. Unenhanced CT scan reveals punctate calcifications in the left adrenal gland (arrow). Note almost complete calcification of the spleen and punctate calcifications in the kidney and lymph nodes.

occur as a result of failure to achieve adequate blood levels of aerosolized pentamidine (43). Unenhanced abdominal CT may reveal punctate or coarse calcifications in the adrenal glands as well as in the spleen, liver, kidneys, and lymph nodes (Fig 20) (43).

Abscess.—Adrenal abscesses are rare, and most have been found in neonates with preexisting adrenal hemorrhage (44). In the setting of suspected neonatal hematomas, US is the imaging modality of choice. Along with the patient's clinical course, failure of an adrenal hematoma to resolve on serial images should indicate the need for further evaluation with aspiration and drainage under US or CT guidance. Contrast-enhanced CT typically shows a thick-walled cystic mass in the gland (45).

• Nonfunctioning Benign Tumors

Nonfunctioning Cortical Adenoma.—Cortical adenomas are incidental findings in 9% of autopsy patients (6). Most such lesions can be further characterized noninvasively; biopsy is reserved for atypical cases. Such adenomas tend to be round or oval, are usually less than 3 cm in diameter, and have homogeneously decreased attenuation with a smooth, well-defined margin.

Cortical adenomas frequently contain a large amount of intracytoplasmic lipid, which allows quantitative analysis of the lesion with attenuation measurements at unenhanced CT (46). In a series of 124 patients with 135 adrenal masses, lesions with an attenuation of less than 18 HU on unenhanced CT scans were all shown to be adenomas (9). On the basis of their review of previously published series combined with their own results, Korobkin et al (9), using a threshold of 10 HU, found an overall sensitivity of 73% and a specificity of 96%. Thus, they concluded that further workup is unnecessary when the lesion has an attenuation of 10 HU or less.

Unfortunately, most adrenal masses are detected on contrast-enhanced CT scans because most abdominal CT procedures are performed after intravenous administration of contrast material. However, even in this setting, Korobkin et al (10) have shown that lesions with an attenuation of less than 30 HU on CT scans obtained 1 hour after contrast material injection

a.

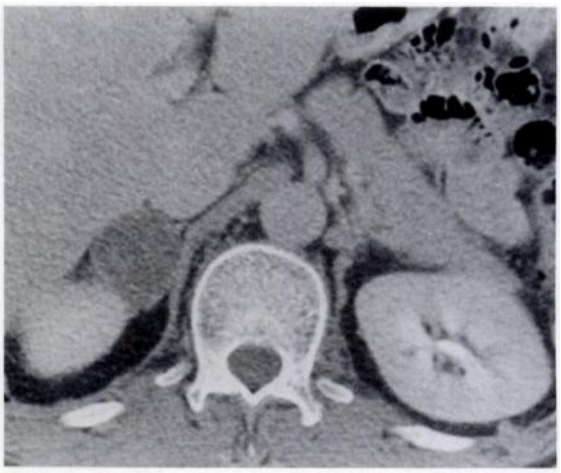

b.

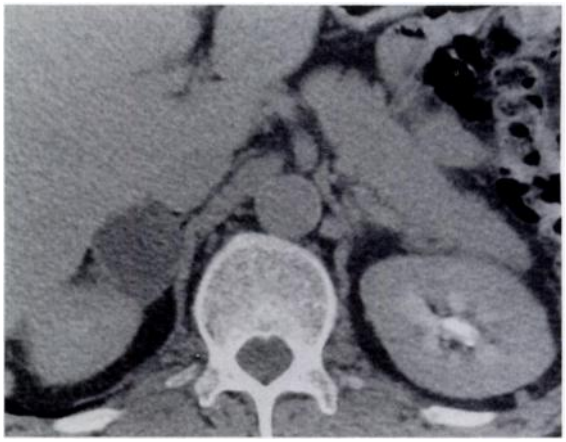

c.

Figure 21. Adenoma in a 63-year-old man. **(a)** Contrast-enhanced helical CT scan obtained during the corticomedullary junction phase shows an indeterminate mass of the right adrenal gland with an attenuation of 29 HU. **(b, c)** Delayed CT scans obtained 15 minutes **(b)** and 70 minutes **(c)** after intravenous administration of contrast material show the mass with an attenuation of 11 HU and −8 HU, respectively.

most likely represent benign adenomas because they demonstrate faster contrast material washout and lower postenhancement attenuation (Fig 21) than do other solid adrenal lesions. More recent studies have shown that differentiation of adenomas from nonadenomas is possible as early as 5–15 minutes after contrast material injection (10,47–50). Lesion attenuation measurement at dynamic contrast-enhanced CT performed less than 180 seconds after starting intravenous administration of contrast material has not proved useful in differentiating adenomas from metastases because there is considerable overlap between the two groups (10,47–50). Performing early delayed CT is an attractive alternative to scheduling separate unenhanced CT or magnetic resonance (MR) imaging when an adrenal mass is found at routine contrast-enhanced CT. Delayed contrast-enhanced CT should be performed if the lesion has an attenuation of more than 10 HU at unenhanced CT or if the mass is indeterminate at chemical shift MR imaging. If the mass has an attenuation of more than 37 HU, further evaluation by means of percutaneous biopsy or surgical excision is usually indicated.

The absence of fat in an adrenal mass does not preclude the diagnosis of adenoma because some adenomas do not contain demonstrable fat. Biopsy may be indicated for lesions 2 cm or more in diameter to exclude metastasis in patients with known extraadrenal primary neoplasms.

Atypical adrenal adenomas may be difficult to differentiate from adrenal cortical adenocarcinomas, particularly if they are more than 5 cm in diameter or demonstrate tumor calcifications (Fig 22) or if intratumoral hemorrhage or necrosis is present (Fig 23). Fine-needle biopsy may have limited value in differentiating adenoma from well-differentiated adenocarcinoma because of their similar cytologic findings.

However, distinguishing cortical adenomas from cysts and ganglioneuromas remains difficult because of their low attenuation at unenhanced CT. An adrenal cyst can be diagnosed

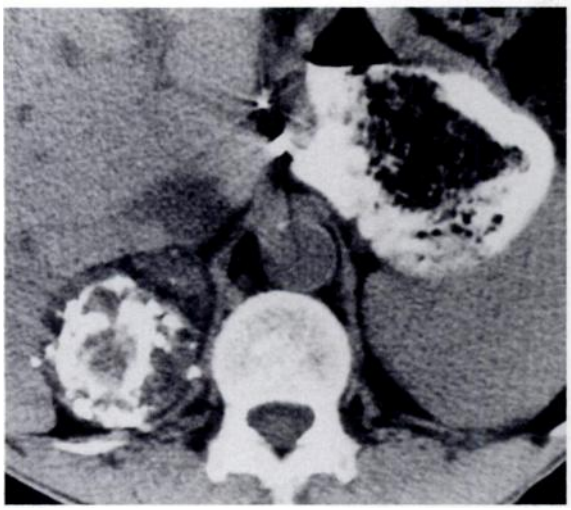

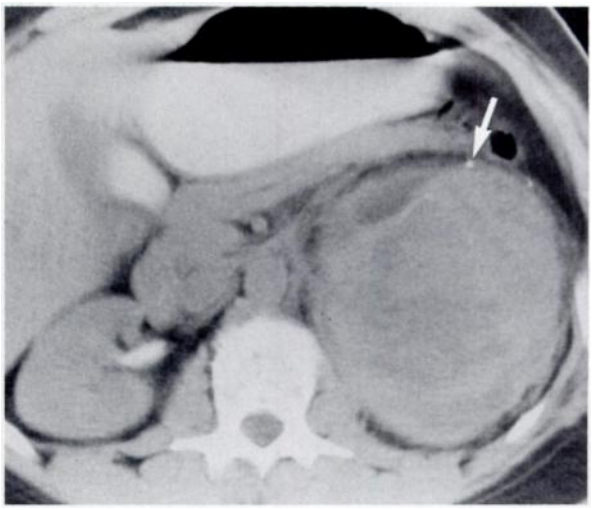

22. 23.

Figures 22, 23. **(22)** Surgically proved calcified adrenal adenoma in a 65-year-old man. Unenhanced CT scan reveals a large right adrenal mass containing coarse calcifications. **(23)** Surgically proved adrenal adenoma with intratumoral hemorrhage in a 48-year-old woman. CT scan obtained after an excretory urogram (not shown) reveals a large cystic mass containing areas of increased attenuation. Note the flecks of calcification at the wall (arrow).

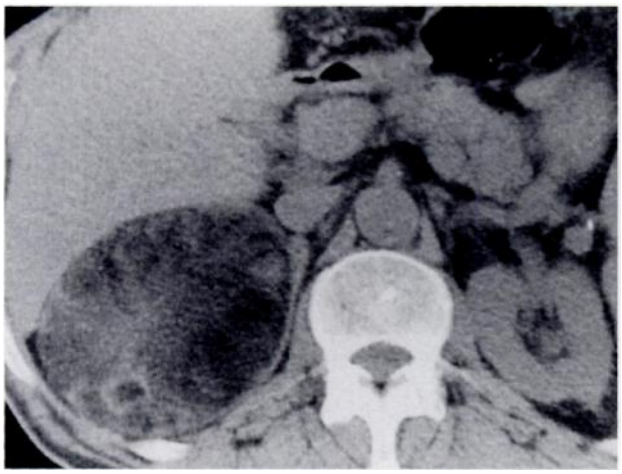

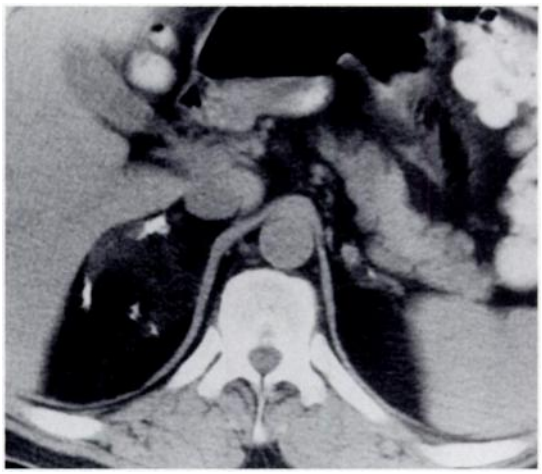

24. 25.

Figures 24, 25. **(24)** Myelolipoma in a 59-year-old man with a history of squamous cell carcinoma of the lung. Unenhanced CT scan demonstrates a 7.5 × 10-cm soft-tissue-attenuation mass containing predominantly fatty components. **(25)** Myelolipoma in a 45-year-old man with a history of chronic renal insufficiency. Unenhanced CT scan shows a well-defined fatty mass of the right adrenal gland with coarse calcifications.

because of its thin-walled, rimlike calcification and the absence of contrast enhancement.

Myelolipoma.—Myelolipomas are usually asymptomatic masses composed of mature fat and bone marrow. Symptoms may occasionally result from hemorrhage within the mass or from mass effect if the lesion is large (51). Myelolipomas may occasionally be bilateral but are usually unilateral and have no side predilection. Calcification occurs in up to 20% of cases and may be related to previous hemorrhage (52).

The CT appearance of myelolipomas depends on their histologic composition and ranges from a fat-dominant mass to a completely nonfatty soft-tissue mass (Figs 24, 25).

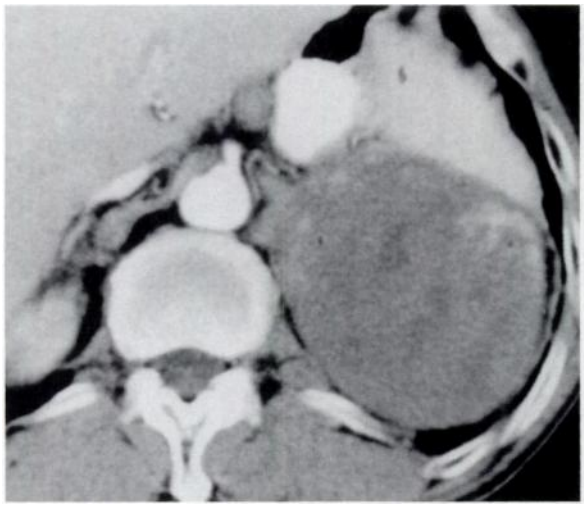

a.

b.

c.

Figure 26. Surgically proved hemangioma in a 69-year-old man. **(a)** Contrast-enhanced helical CT scan reveals a large soft-tissue-attenuation mass of the left adrenal gland with peripheral areas of enhancement. **(b)** Delayed CT scan demonstrates heterogeneous enhancement. **(c)** Left infraphrenic angiogram (arterial phase) reveals pooling of contrast material in the periphery of the mass. Persistent pooling of contrast material was also present during the venous phase (not shown).

In most cases, however, CT reveals a well-defined suprarenal mass with a fine capsule and containing areas of fat. The mass typically has an attenuation ranging from −30 to −115 HU, significantly lower than the attenuation of cortical adenomas (52,53). The tumor may contain small calcifications (Fig 25). Enhancement is observed in the soft-tissue component of myelolipomas after intravenous administration of contrast material and may mask the fat attenuation. When the tumor has bled, CT may show high- or low-attenuation fluid collections depending on the age of the blood. In equivocal cases, a definitive diagnosis can be made with CT-guided needle biopsy to confirm the presence of mature adipose tissue and normal hematopoietic tissue.

Hemangioma.—Adrenal hemangiomas are rare benign tumors of the adrenal gland; less than 30 cases have been reported in the literature. Typically, adrenal hemangiomas are discovered incidentally and are more than 10 cm in diameter (54,55).

At unenhanced CT, adrenal hemangiomas appear as a well-delineated hypoattenuating or heterogeneously attenuating mass (54–57). Calcification may be present in approximately two-thirds of cases. Irregular or crescent calcification from a previous hemorrhage or from thrombosis or necrosis may be present. The presence of phleboliths within the lesion is characteristic of a hemangioma. After intravenous bolus administration of contrast material, CT shows multiple peripheral nodular areas of marked enhancement corresponding to angiographic findings and persistent pooling of contrast material at the periphery of the lesion (Fig 26). However, a filling-in phenomenon, frequently described in cavernous hemangioma of the liver, may also rarely occur in adrenal he-

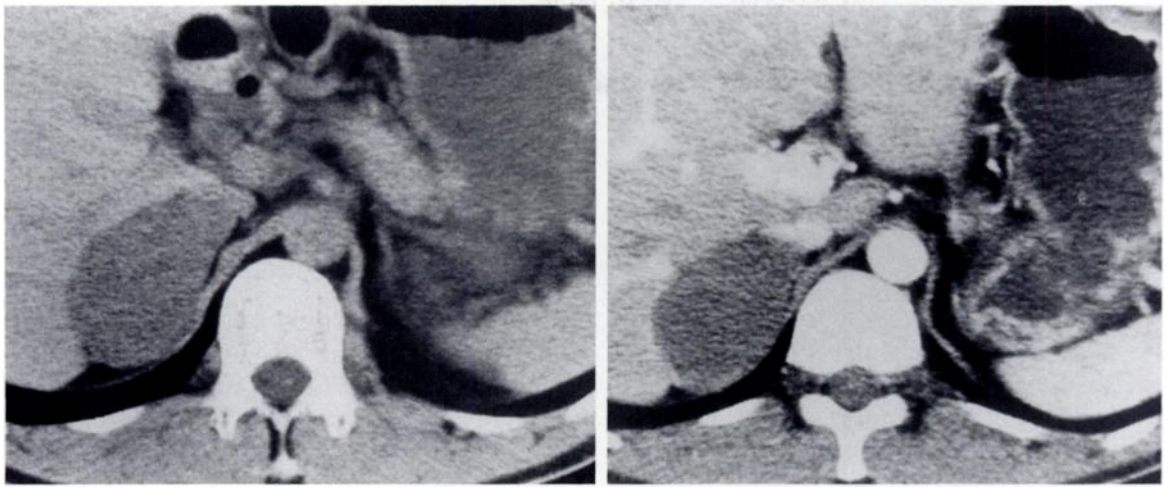

a. b.

c.

Figure 27. Surgically proved ganglioneuroma in a 40-year-old man. **(a)** Unenhanced CT scan reveals a well-defined hypoattenuating mass of the right adrenal gland relative to muscle. **(b)** Contrast-enhanced helical CT scan shows minimal enhancement. Water was administered orally as a negative contrast material. **(c)** Fat-saturated spin-echo T2-weighted (repetition time msec/echo time msec = 2,000/70) MR image demonstrates a hyperintense mass relative to the liver. A spin-echo T1-weighted MR image (not shown) showed the mass to be isointense relative to the liver.

mangioma because of the presence of necrosis, fibrosis, and thrombosis in the center of the tumor.

Ganglioneuroma.—Ganglioneuromas are tumors arising from sympathetic ganglia. Forty-one percent of abdominal ganglioneuromas occur in the adrenal glands (58). Patients with neurogenic tumors arising from sympathetic ganglia (ie, neuroblastoma, ganglioneuroblastoma, ganglioneuroma) occasionally present with diarrhea, sweating, hypertension, virilization, or myasthenia gravis (58). At histologic analysis, ganglioneuroblastomas exhibit a degree of differentiation that is intermediate between those of neuroblastomas and ganglioneuromas and are potentially malignant. Ganglioneuromas are better differentiated than ganglioneuroblastomas and occur in older children and adults.

At CT, ganglioneuromas appear as well-defined masses (59–61). In a recent series by Radin et al (60), ganglioneuromas appeared homogeneous and hypoattenuating relative to muscle on both unenhanced and contrast-enhanced CT scans (Fig 27). After intravenous administration of contrast material, some degree of heterogeneity may be seen in large lesions. Calcification may also be present. Either CT-guided biopsy or surgical resection is required to confirm benignity.

■ ADDISON DISEASE

Addison disease may be either acute, subacute, or chronic (62). Acute Addison disease is rare and may result from bilateral adrenal hemorrhage (adrenal apoplexy), which is usually due to severe shock and sepsis or occasionally to a hemorrhagic diathesis (30). Bilateral traumatic adrenal hematomas occasionally result in adrenal insufficiency, which occurs a few weeks to months after the trauma. In this setting, the

demonstration of bilateral adrenal hematomas at CT may be the first clue to the diagnosis because the clinical manifestations are not specific for the diagnosis.

Disease that has been present for less than 2 years is defined as a subacute form of Addison disease. CT plays a critical role in the evaluation of such cases, typically revealing enlargement of both adrenal glands, with necrotic centers and a rim of contrast enhancement (42,63) (Fig 19). CT-guided biopsy is indicated to establish a cause that may include active adrenalitis secondary to tuberculosis, histoplasmosis, and other fungi. Appropriate therapy for specific organisms and direct hormone replacement can be initiated.

CT provides little information in patients with chronic Addison disease compared with the acute and subacute forms. However, CT may suggest the cause of disease in such cases (63,64). Idiopathic atrophy, probably due to autoimmune disorder, is the most common cause of chronic Addison disease in the United States, followed by previous granulomatous adrenalitis secondary to tuberculosis and histoplasmosis. CT findings in idiopathic Addison disease include small, atrophic remnants of the adrenal glands bilaterally without calcification; in practice, however, it is difficult to tell whether the normally small adrenal glands are atrophic. At plain radiography, calcification is present in one or both adrenal glands in 25% of patients with Addison disease (65). Calcifications have been reported to be present at CT in 50% of patients with Addison disease secondary to tuberculosis (64). However, bilateral adrenal calcifications are not pathognomonic for previous granulomatous adrenalitis and are radiologically indistinguishable from idiopathic calcifications and calcifications from previous adrenal hemorrhage (Fig 17). Clinical and hormonal correlation is essential because adrenal glands with irregular calcifications may have preserved adrenal function (62,66).

■ CONCLUSIONS

CT plays a significant role in the radiologic evaluation of adrenal lesions. In most cases, CT can be used to make a specific diagnosis and to guide appropriate management. Thin-section helical CT is highly accurate in the localization of an adrenal mass in patients with diseases associated with hyperfunctioning adrenal glands. A specific diagnosis of acute or subacute adrenal hematoma or myelolipoma can be established with CT. In addition, CT is useful in the evaluation of patients with Addison disease, particularly when the disease is secondary to disseminated histoplasmosis and tuberculosis. Attenuation of 10 HU or less at unenhanced CT usually helps differentiate a benign cortical adenoma from metastasis. Delayed contrast-enhanced CT performed as early as 5-15 minutes after intravenous administration of contrast material may allow differential diagnosis of an indeterminate mass at unenhanced CT or chemical shift MR imaging. If the mass has an attenuation of more than 37 HU, CT-guided biopsy or surgical removal is required.

■ REFERENCES

1. Dunnick NR. Adrenal imaging: current status. AJR 1990; 154:927-936.
2. Choyke P. Imaging of the adrenal gland. In: McClennan BL, ed. Syllabus: a categorical course in genitourinary radiology. Oak Brook, Ill: Radiological Society of North America, 1994; 71-78.
3. Kloos RT, Gross MD, Francis IR, Korobkin M, Shapiro B. Incidentally discovered adrenal masses. Endocr Rev 1995; 16:460-484.
4. Korobkin M, Francis IR, Kloos RT, Dunnick NR. The incidental adrenal mass. Radiol Clin North Am 1996; 34:1037-1054.
5. Dunnick NR, Doppman JL, Gill JR Jr, Strott CA, Keiser HR, Brennan MF. Localization of functional adrenal tumors by computed tomography and venous sampling. Radiology 1982; 142:429-433.
6. Dunnick NR, Korobkin M, Francis I. Adrenal radiology: distinguishing benign from malignant adrenal masses. AJR 1996; 167:861-867.
7. Lee MJ, Hahn PF, Papanicolaou N, et al. Benign and malignant adrenal masses: CT distinction with attenuation coefficients, size, and observer analysis. Radiology 1991; 179:415-418.
8. van Erkel AR, van Gils APG, Lequin M, Kruitwagen C, Bloem JL, Falke THM. CT and MR distinction of adenomas and nonadenomas of the adrenal glands. J Comput Assist Tomogr 1994; 18:432-438.
9. Korobkin M, Brodeur FJ, Yutzy GG, et al. Differentiation of adrenal adenomas from nonadenomas using CT attenuation values. AJR 1996; 166:531-536.
10. Korobkin M, Brodeur FJ, Francis IR, Quint LE, Dunnick NR, Goodsitt M. Delayed enhanced CT for differentiation of benign from malignant adrenal masses. Radiology 1996; 200:737-742.

11. Doppman JL, Miller DL, Dwyer AJ, et al. Macronodular adrenal hyperplasia in Cushing disease. Radiology 1988; 166:347-352.
12. Doppman JL, Nieman LK, Travis WD, et al. CT and MR imaging of massive macronodular adrenocortical disease: a rare cause of autonomous primary adrenal hypercortisolism. J Comput Assist Tomogr 1991; 15:773-779.
13. Doppman JL, Travis WD, Nieman L, et al. Cushing syndrome due to pigmented nodular adrenocortical disease: findings at CT and MR imaging. Radiology 1989; 172:415-420.
14. Doppman JL, Nieman L, Miller DL, et al. Ectopic adrenocorticotropic hormone syndrome: localization studies in 28 patients. Radiology 1989; 172:115-124.
15. Dunnick NR, Leight GS Jr, Roubidoux MA, et al. CT in the diagnosis of primary aldosteronism: sensitivity in 29 patients. AJR 1993; 160:321-324.
16. Miyake H, Maeda H, Tashiro M, et al. CT of adrenal tumors: frequency and clinical significance of low-attenuation lesions. AJR 1989; 152:1005-1007.
17. Doppman JL, Gill JR Jr. Hyperaldosteronism: sampling the adrenal veins. Radiology 1996; 198:309-312.
18. Radin DR, Manoogian C, Nadler JL. Diagnosis of primary hyperaldosteronism: importance of correlating CT findings with endocrinologic studies. AJR 1992; 158:553-557.
19. Neumann HPH, Berger DP, Sigmund G, et al. Pheochromocytomas, multiple endocrine neoplasia type 2, and von Hippel-Lindau disease. N Engl J Med 1993; 329:1531-1538.
20. Raisanen J, Shapiro B, Glazer GM, Desai S, Sisson JC. Plasma catecholamines in pheochromocytoma: effect of urographic contrast media. AJR 1984; 143:43-46.
21. Radin DR, Ralls PW, Boswell WD Jr, Colletti PM, Lapin SA, Halls JM. Pheochromocytoma: detection by unenhanced CT. AJR 1986; 146:741-744.
22. Mukherjee JJ, Peppercorn PD, Reznek RH, et al. Pheochromocytoma: effect of non-ionic contrast medium in CT on circulating catecholamine levels. Radiology 1997; 202:227-231.
23. Burks DW, Mirvis SE, Shanmuganathan K. Acute adrenal injury after blunt abdominal trauma: CT findings. AJR 1992; 158:503-507.
24. Sevitt S. Post-traumatic adrenal apoplexy. J Clin Pathol 1955; 8:185-194.
25. Sivit CJ, Ingram JD, Taylor GA, Bulas DI, Kushner DC, Eichelberger MR. Posttraumatic adrenal hemorrhage in children: CT findings in 34 patients. AJR 1992; 158:1299-1302.
26. Gomez RG, McAninch JW, Carroll PR. Adrenal gland trauma: diagnosis and management. J Trauma 1993; 35:870-874.
27. Kenney PJ, Stanley RJ. Calcified adrenal masses. Urol Radiol 1987; 9:9-15.
28. Mody MK, Kazerooni EA, Korobkin M. Percutaneous CT-guided biopsy of adrenal masses: immediate and delayed complications. J Comput Assist Tomogr 1995; 19:434-439.
29. Bowen A, Keslar P, Newman B, Hashida Y. Adrenal hemorrhage after liver transplantation. Radiology 1990; 176:85-88.
30. Wolverson MK, Kannegiesser H. CT of bilateral adrenal hemorrhage with acute adrenal insufficiency in the adult. AJR 1984; 142:311-314.
31. Ling D, Korobkin M, Silverman PM, Dunnick NR. CT demonstration of bilateral adrenal hemorrhage. AJR 1983; 141:307-308.
32. Hoeffel C, Legmann P, Luton JP, Chapuis Y, Fayet-Boynnin P. Spontaneous unilateral adrenal hemorrhage: computerized tomography and magnetic resonance imaging findings in 8 cases. J Urol 1995; 154:1647-1651.
33. Rumancik M, Bosniak AB. Miscellaneous conditions of the adrenals and adrenal pseudotumors. In: Pollack HM, ed. Clinical urography. 1st ed. Philadelphia, Pa: Saunders, 1990; 2399-2412.
34. Tung GA, Pfister RC, Papanicolau N, Yoder IC. Adrenal cysts: imaging and percutaneous aspiration. Radiology 1989; 173:107-110.
35. Rozenblit A, Morehouse HT, Amis ES Jr. Cystic adrenal lesions: CT features. Radiology 1996; 201;541-548.
36. Sakamoto I, Nakahara N, Fukuda T, Nagayoshi K, Matsunaga N, Hayashi K. Atypical appearance of adrenal pseudocysts. J Urol 1994; 152:150-152.
37. Wilms GE, Baert AL, Kint EJ, Pringot JH, Goddeeris PG. Computed tomographic findings in bilateral adrenal tuberculosis. Radiology 1983; 146:729-730.
38. Buxi TB, Vohra RB, Sujatha Y, Byotra SP, Mukherji S, Daniel M. CT in adrenal enlargement due to tuberculosis: a review of literature with five new cases. Clin Imaging 1992; 16:102-108.
39. Radin DR. Disseminated histoplasmosis: abdominal CT findings in 16 patients. AJR 1991; 157:955-958.
40. Sarosi GA, Voth DW, Dahl BA, Doto IL, Tosh FE. Disseminated histoplasmosis: results of long-term follow-up: a Center for Disease Control cooperative mycoses study. Ann Intern Med 1971; 75:511-516.
41. Levine E. CT evaluation of acute adrenal histoplasmosis. Urol Radiol 1991; 13:103-106.
42. Wilson DA, Muchmore HG, Tisdal RG, Fahmy A, Pitha JV. Histoplasmosis of the adrenal glands studied by CT. Radiology 1984; 150: 779-783.

43. Radin DR, Baker EL, Klatt EC, et al. Visceral and nodal calcification in patients with AIDS-related *Pneumocystis carinii* infection. AJR 1990; 154:27-31.
44. Atkinson GO Jr, Kodroff MB, Gay BB Jr, Ricketts RR. Adrenal abscess in the neonate. Radiology 1985; 155:101-104.
45. O'Brien WM, Choyke PL, Copeland J, Klappenbach RS, Lynch JH. Computed tomography of adrenal abscess. J Comput Assist Tomogr 1987; 11:550-551.
46. Korobkin M, Giordano TJ, Brodeur FJ, et al. Adrenal adenomas: relationship between histologic lipid and CT and MR findings. Radiology 1996; 200:743-747.
47. Korobkin MT, Brodeur FJ, Francis IR, Quint LE, Dunnick NR. Contrast enhancement washout characteristics of adrenal adenomas at CT (abstr). Radiology 1996; 201(P):187.
48. Boland GW, Hahn PF, Peña C, Mueller PR. Adrenal masses: characterization with delayed contrast-enhanced CT. Radiology 1997; 201: 693-696.
49. Szolar DH, Kammerhuber F. Quantitative CT evaluation of adrenal gland masses: a step forward in the differentiation between adenomas and nonadenomas? Radiology 1997; 202:517-521.
50. Korobkin M, Brodeur FJ, Francis IR, Quint LE, Dunnick NR, Londy F. Time-attenuation curves of adrenal adenomas and metastases following CT contrast enhancement. Presented at the annual meeting of the Society of Uroradiology, Santa Fe, NM, 1997.
51. Albala DM, Memoli VA, Chung CJ, Heaney JA, Sueoka BL. Hemorrhagic myelolipoma of the adrenal gland after blunt trauma. Urology 1991; 38:559-561.
52. Musante F, Derchi LE, Zappasodi F, et al. Myelolipoma of the adrenal gland: sonographic and CT features. AJR 1988; 151:961-964.
53. Cyran KM, Kenney PJ, Memel DS, Yacoub I. Adrenal myelolipoma. AJR 1996; 166:395-400.
54. Gaudio AD, Solidoro G, Martinelli G. Adrenal hemangiomas: two case reports with a review of the literature. Surgery 1989; 105:674-681.
55. Sabanegh E Jr, Harris MJ, Grider D. Cavernous adrenal hemangioma. Urology 1993; 42:327-330.
56. Derchi LE, Rapaccini GL, Banderali A, Danza FM, Grillo F. Ultrasound and CT findings in two cases of hemangioma of the adrenal gland. J Comput Assist Tomogr 1989; 13:659-661.
57. Deckers F, De Schepper A, Shamsi K, Hauben E, Van Marck E. Cavernous hemangioma of the adrenal gland: CT appearance. J Comput Assist Tomogr 1993; 17:506-507.
58. Enzinger FM, Weis SW. Primitive neuroectodermal tumors and related lesions. In: Enzinger FM, Weiss SW, eds. Soft tissue tumors. 3rd ed. St Louis, Mo: Mosby-Year Book, 1995; 929-964.
59. Bosniak MA. Neoplasms of the adrenal medulla. In: Pollack HM, ed. Clinical urography. 1st ed. Philadelphia, Pa: Saunders, 1990; 2344-2346.
60. Radin R, David CL, Goldfarb H, Francis IR. Adrenal and extraadrenal retroperitoneal ganglioneuroma: imaging findings in 13 adults. Radiology 1997; 201:703-707.
61. Johnson GL, Hruban RH, Marshall FF, Fishman EK. Primary adrenal ganglioneuroma: CT findings in four patients. AJR 1997; 169:169-171.
62. Doppman JL. Adrenal cortical insufficiency. In: Pollack HM, ed. Clinical urography. 1st ed. Philadelphia, Pa: Saunders, 1990; 2338-2343.
63. Doppman JL, Gill JR Jr, Nienhuis AW, Earl JM, Long JA Jr. CT findings in Addison's disease. J Comput Assist Tomogr 1982; 6:757-761.
64. Sawczuk IS, Reitelman C, Libby C, Grant D, Vita J, White RD. CT findings in Addison's disease caused by tuberculosis. Urol Radiol 1986; 8:44-45.
65. Jarvis JL, Jenkins D, Sosman MC, Thorn GW. Roentgenologic observations in Addison's disease: a review of 120 cases. Radiology 1954; 62:16-28.
66. Vita JA, Silverberg SJ, Goland RS, Austin JHM, Knowlton AI. Clinical clues to the cause of Addison's disease. Am J Med 1985; 78:461-466.

This article meets the criteria for 1.0 credit hour in category 1 of the AMA Physician's Recognition Award. To obtain credit, see the questionnaire on pp 451-456.